Virology 526 (2019) 146–154

Contents lists available at ScienceDirect

Virology

journal homepage: www.elsevier.com/locate/virology

Evaluation of antiviral therapies in respiratory and neurological disease models of Enterovirus D68 infection in mice

Brett L. Hurst[a,b], W. Joseph Evans[a,b], Donald F. Smee[a,b], Arnaud J. Van Wettere[b,c], E. Bart Tarbet[a,b,c,*]

[a] Institute for Antiviral Research, Utah State University, Logan, UT, United States
[b] Department of Animal, Dairy and Veterinary Sciences, Utah State University, Logan, UT, United States
[c] Utah Veterinary Diagnostic Laboratory, Logan, UT, United States

ARTICLE INFO

Keywords:
Enterovirus D68
Animal model
Respiratory disease
Neurological disease
Acute flaccid myelitis
Antiviral
Guanidine

ABSTRACT

Enterovirus D68 (EV-D68) is unique among enteroviruses because of the ability to cause severe respiratory disease as well as neurological disease. We developed separate models of respiratory and neurological disease following EV-D68 infection in AG129 mice that respond to antiviral treatment with guanidine. In four-week-old mice infected intranasally, EV-D68 replicates to high titers in lung tissue increasing the proinflammatory cytokines MCP-1 and IL-6. The respiratory infection also produces an acute viremia. In 10-day-old mice infected intraperitoneally, EV-D68 causes a neurological disease with weight-loss, paralysis, and mortality. In our respiratory model, treatment with guanidine provides a two-log reduction in lung virus titers, reduces MCP-1 and IL-6, and prevents histological lesions in the lungs. Importantly, viremia is prevented by early treatment with guanidine. In our neurological model, guanidine treatment protects mice from weight-loss, paralysis, and mortality. These results demonstrate the utility of these models for evaluation of antiviral therapies for EV-D68 infection.

1. Introduction

Enterovirus D68 (EV-D68) is a non-enveloped, single-stranded, positive sense RNA virus of the family *Picornaviridae*. Despite identification in 1962, disease outbreaks were not widely reported until the early 2000s. Beginning with an outbreak of severe acute respiratory disease in the Philippines in 2008–2009, an increase in confirmed cases of EV-D68 infection in children led to the classification of EV-D68 as a re-emerging pathogen (Imamura and Oshitani, 2015). In the late summer and early fall of 2014 an outbreak of EV-D68 occurred in the United States. According to the Centers for Disease Control and Prevention (CDC), laboratories confirmed a total of 1153 cases of EV-D68 respiratory infection in 49 states and the District of Columbia (Control CfD). Despite being the largest outbreak of EV-D68 ever recorded, it is likely that millions were infected but never tested (Messacar et al., 2016a). Retrospective studies concluded that EV-D68 infections significantly burdened hospitals in the United States due to the magnitude of the outbreak (Messacar et al., 2016b).

In addition to causing severe respiratory disease, the 2014 outbreak was also temporally associated with an increase in cases of acute flaccid paralysis (AFP) both in the United States and Canada (Maloney et al., 2015; Messacar et al., 2015; Yea et al., 2017). Cases of acute flaccid paralysis are routinely monitored and reported to the World Health Organization (WHO) for the detection of wild poliovirus in circulation (Tangermann et al., 2017). Where AFP is defined by the WHO as the "sudden onset of paralysis/weakness in any part of the body of a child less than 15 years old" (World Health Organization, 2003), acute flaccid myelitis (AFM) is a syndrome of AFP and is further defined by the CDC as occurring in patients younger than 21 years old, with one or more limbs demonstrating weakness or paralysis, and spinal cord lesions observed during magnetic resonance imaging (MRI) (Nelson et al., 2016). Both AFP and AFM have been used to describe the neurological illness associated with EV-D68 infection (Messacar et al., 2015; Aliabadi et al., 2016; Esposito et al., 2015, 2017; Greninger et al., 2015; Hovden and Pfeiffer, 2015; Lang et al., 2014; Mirand and Peigue-Lafeuille, 2015; Pfeiffer et al., 2015). For the purposes of this paper, AFM will be used to describe the paralysis induced by EV-D68 infection.

AFM was identified by the CDC in a total of 120 children infected with EV-D68 from 34 states between August and December of 2014 (Aliabadi et al., 2016; Greninger et al., 2015). Since that time, cases of AFM have been associated with EV-D68 infection in France, Norway and the United Kingdom (Lang et al., 2014; Pfeiffer et al., 2015; Crone

* Correspondence to: Utah State University, Logan, UT, United States.
E-mail address: bart.tarbet@usu.edu (E.B. Tarbet).

https://doi.org/10.1016/j.virol.2018.10.014
Received 4 June 2018; Received in revised form 14 October 2018; Accepted 15 October 2018
Available online 31 October 2018
0042-6822/

et al., 2016; Varghese et al., 2015; Williams et al., 2016). In addition, several children diagnosed with AFM had neurologic deficits 12 months after the original infection (Yea et al., 2017).

Here we describe two separate models of EV-D68 infection in mice that model human respiratory and neurological disease and respond to treatment with antiviral therapy. Both models utilize AG129 mice that are deficient in interferon (IFN)- α/β and –γ receptors (Muller et al., 1994; van den Broek et al., 1995), making the mice more permissive to EV-D68 infection. While mice with intact IFN signaling have shown EV-D68-associated disease, this was only shown in mice less than two days old (Hixon et al., 2017a). In addition, two-day-old mice developed neurological disease, but not respiratory disease. The NIH funding for development of these models specified the use of AG129 mice, although we also evaluated infection of BALB/c, C57BL/6J, FVB/NJ, SJL/J, and Swiss-Webster mice. Only AG129 mice showed respiratory and neurological disease signs following infection with mouse-adapted EV-D68. In addition, AG129 mice have been used for development of other virus infection models, including Tacaribe arenavirus (Gowen et al., 2010), Dengue virus (Julander et al., 2011), Zika virus (Julander and Siddharthan, 2017), and have even been used in vaccine evaluations in Dengue virus models (Sarathy et al., 2015). It has been observed that the IFN response in human infections is attenuated by EV-D68 infection (Xiang et al., 2014, 2015; Rui et al., 2017). Therefore, the use of interferon deficient mice was considered acceptable, although not ideal for model development.

The respiratory model developed in four-week-old mice includes an intranasal challenge with mouse-adapted EV-D68 (US/MO/14–18949). The subsequent infection is characterized by viremia, altered lung function (PenH) as demonstrated by plethysmography, high viral titers and pro-inflammatory cytokines in lung tissue, and histological changes including interstitial pneumonia (Evans et al., 2018). The neurological model in ten-day-old mice includes an intraperitoneal challenge with mouse-adapted EV-D68. The subsequent infection leads to a systemic viremia with viral titers observed in leg muscle, spinal cord, and brain followed by paralysis and mortality. These studies evaluated the antiviral effects of guanidine, an inhibitor of the 2C protein function, in both respiratory and neurological disease models of EV-D68 infection.

2. Materials and methods

2.1. Virus and cells

Enterovirus D68 (US/MO/14–18949) was obtained from the American Type Culture Collection (ATCC, Manassas, VA). This virus was serially-passaged 30 times in the lungs of AG129 mice to increase its virulence (Evans et al., 2018). After passaging, the virus was plaque-purified three times and amplified in RD cells to obtain a working stock. Human rhabdomyosarcoma (CCL-136) cells (RD) from ATCC were cultured in 5% fetal bovine serum (FBS) and minimum essential media (MEM) (GE Healthcare Hyclone, Logan, UT USA). Media used for EV-D68 cell culture infection was 2% FBS and 25 mM $MgCl_2$ in MEM + 50 μg/ml of gentamicin. Tissues harvested from mice were homogenized in MEM. MEM served as the vehicle for animal infections.

2.2. Animals

Male and female AG129 mice were obtained from a specific-pathogen-free breeding colony at Utah State University. For the respiratory model, four-week-old, male and female mice were used for all studies. For the neurological model, 10-day-old male and female AG129 mice were infected without being removed from the dam.

2.3. Antiviral compounds

Guanidine HCl was purchased from Sigma-Aldrich (St. Louis, MO).

2.4. Virus titer

Tissue virus titers were determined on RD cells in 96-well microplates. Plates were seeded with cells 24 h prior to infection and incubated at 37 °C and 5% CO_2. Tissue samples were harvested and homogenized in 1 ml MEM and frozen until titration. Serial 10-fold dilutions of tissue samples were prepared and added to four replicate wells containing RD cells. Microplates were incubated for 6 days at 33 °C with 5% CO_2 (Smee et al., 2016). Plates were examined visually six days' post-infection for viral cytopathic effects. The 50% cell culture infectious doses ($CCID_{50}$) were calculated using an endpoint dilution method (Reed, 1938) and virus titers reported per ml.

2.5. Histopathology

For each mouse, the entire left lung was removed and fixed in freshly prepared 4% paraformaldehyde for 2 days. Paraformaldehyde-fixed tissue sections were processed and embedded in paraffin according to routine histologic techniques. Sections, 5 μm thick, were stained with hematoxylin and eosin (H&E) and examined by light microscopy by a board certified veterinary pathologist. Lesions were graded on the following scale of 0–4: 0 = no lesions, 1 = minimal lesions, 2 = mild lesions, 3 = moderate lesions, and 4 = severe lesions.

2.6. Lung cytokine/chemokine determinations

A sample (20 μl) from each lung homogenate was tested for cytokines and chemokines using an ELISA-based assay according to the manufacturer's instructions (Quansys Biosciences Q-Plex™ Array, Logan, UT). The Quansys multiplex ELISA is a quantitative test in which 16 distinct capture antibodies have been applied to each well of a 96-well plate in a defined array. Each sample supernatant was tested at 2 dilutions for the following: IL-1α, IL-1β, IL-2, IL-3, IL-4, IL-5, IL-6, IL-10, IL-12p70, IL-17, MCP-1, IFN-γ, TNFα, MIP-1α, GM-CSF, and RANTES. Cytokine and chemokine titers of mice infected with EV-D68 are reported in pg/ml of homogenized lung tissue. *Definition of abbreviations are: IL - interleukin; MCP - monocyte chemoattractant protein; IFN - interferon; TNF - tumor necrosis factor, MIP – macrophage inflammatory Protein; GM-CSF - granulocyte/ macrophage colony stimulating factor; and RANTES - regulated upon activation, normal T cell expressed and secreted.*

2.7. Evaluation of guanidine in vivo using EV-D68-infected four-week-old mice

Three groups of four-week-old mice (n = 12 per group) were infected intranasally with MEM containing EV-D68 ($1.0 \times 10^{4.5}$ $CCID_{50}$/mouse) in a 90 μl volume. Guanidine treatments started four hours post-infection and continued b.i.d. for 5 days via the intraperitoneal route. Doses of 100 or 200 mg/kg/day of guanidine were used while placebo-treated mice were treated on the same schedule. Physiological sterile saline was used to solubilize guanidine and to treat the placebo group. Four mice per group were euthanized on days one, three, and five post-infection for collection of lung tissue and whole blood. The left lung was used for histopathology and the right lung was used for virus titers and quantification of cytokines. Blood samples were evaluated for viremia.

2.8. Evaluation of lung function by plethysmography

The plethysmograph and mouse sized acquisition chambers (emka Technologies, Falls Church, VA) were used to evaluate lung function. The following parameters were measured and analyzed: enhanced pause (Penh), tidal volume (TV), minute (MV) and expiratory (EV) volumes, times of inspiration (Ti), expiration (Te), and relaxation (RT), peak inspiratory (PIF) and expiratory (PEF) flow, frequency of breath (Freq), 50% expiratory flow (EF50) and end inspiratory (EIP) and

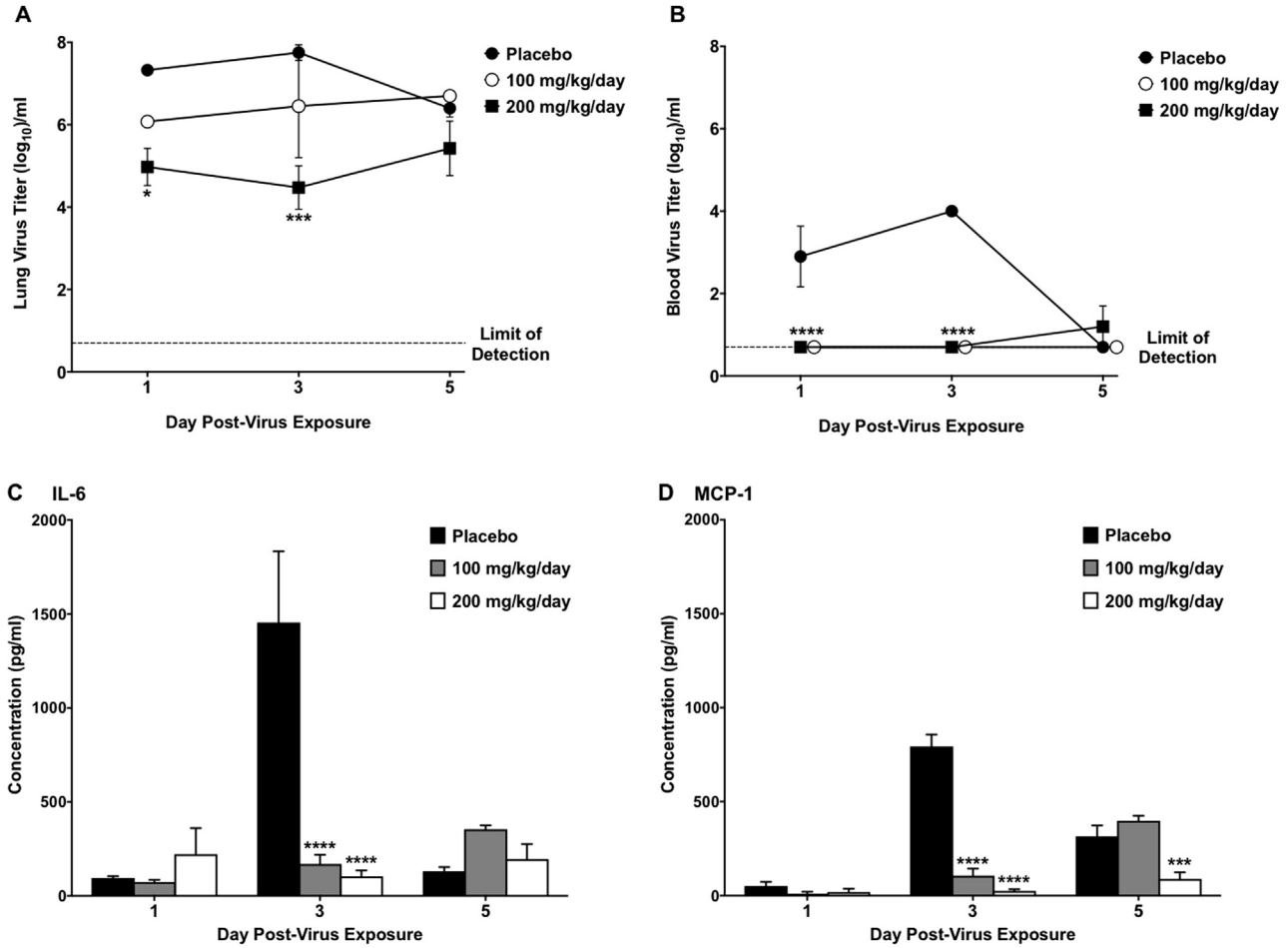

Fig. 1. Lung virus titers and lung cytokine/chemokine concentrations in four-week-old mice infected intranasally with EV-D68 and treated with guanidine. Mice (n = 12/group) were treated b.i.d. × 5 days beginning 4 h post-infection. Graphs represent the mean values and standard error of groups of four mice each. (A) Guanidine reduced lung virus titers in EV-D68-infected mice. (B) Blood virus titers were reduced by guanidine treatment at 100 and 200 mg/kg/day. (C) Increases in IL-6 in lung tissue induced by EV-D68 infection were prevented by guanidine treatment. (D) Guanidine decreased production of MCP-1 in the lungs caused by EV-D68 infection. $^{*}P < 0.05$, $^{***}P < 0.001$, $^{****}P < 0.0001$.

expiratory (EEP) pauses. To reduce variability, mean readings from infected mice were normalized to mean readings from mock-infected (cell culture medium) controls on each day. To obtain measurements, mice were placed in the chambers and allowed to acclimate for three minutes. Plethysmography readings were then recorded for the next five minutes in response to room air. To simulate a hypercapnia challenge, the chambers were flooded with a gas mixture containing 7% CO_2, 50% O_2 and balanced with N_2. The plethysmography readings were recorded for an additional five minutes as CO_2-challenged.

2.9. Evaluation of lung function (Penh) in EV-D68-infected four-week-old mice following treatment with guanidine

Four groups of eight mice were used to evaluate the impact of guanidine on Penh after EV-D68 infection. A mock-infected control group was used as a baseline for evaluation of plethysmography measurements. Infected mice were challenged by intranasal instillation using a 90 µl volume of MEM containing EV-D68 ($1.0 \times 10^{4.5}$ $CCID_{50}$). Guanidine treatments started four hours post-infection and occurred b.i.d. × five days. A dose of 200 mg/kg/day of guanidine was evaluated in this study. Guanidine was solubilized in saline and administered via the intraperitoneal route in a 0.1 ml volume. Placebo-treated mice received saline on the same schedule. Plethysmography readings were obtained on days 1, 3, 5 and 7 post-infection.

2.10. Characterization of EV-D68 in 10-day-old mice

Four groups of six mice each were infected intraperitoneally with EV-D68 using a 50 µl volume of MEM containing one of four dilutions of EV-D68 equating to challenge doses of $1.0 \times 10^{6.7}$, $1.0 \times 10^{6.2}$, $1.0 \times 10^{5.7}$, or $1.0 \times 10^{5.2}$ $CCID_{50}$ of EV-D68. A fifth group was mock-infected using cell culture medium and served as normal controls. Mice were monitored daily for weight-loss, neurological score and mortality.

2.11. Neurological scoring system for EV-D68 infection in mice

To quantify paralysis induced by EV-D68 infection, we adapted a neurological scoring system used in a mouse model for amyotrophic lateral sclerosis (Hatzipetros et al., 2015). However, mice were evaluated only for hind limb function and mobility. An impact on righting reflex was not observed in mice with paralysis.

2.12. In vivo evaluation of guanidine treatment in 10-day-old mice

Groups of five mice were infected intraperitoneally with a 50 µl volume of MEM containing EV-D68 ($1.0 \times 10^{6.7}$ $CCID_{50}$). Four hours post-infection, mice were treated i.p. with guanidine at doses of 12.5, 25, 50 or 100 mg/kg/day. Treatments occurred b.i.d. for five days. Saline was used to solubilize guanidine and as placebo treatment. Mice were monitored daily for weight-loss, neurological score and mortality.

An additional five mice were included in the placebo-treated and the 100 mg/kg/day guanidine treated groups for euthanasia on day three post-infection for tissue virus titers and quantification of cytokines. Lungs, liver, kidney, spleen, leg muscle, spinal cord, and brain tissue were collected and evaluated for tissue virus titers.

2.13. Ethical treatment of animals

This study was done under the approval of the Institutional Animal Care and Use Committee of Utah State University. The work was completed in the AAALAC-accredited Laboratory Animal Research Center of Utah State University in accordance to the National Institutes of Health Guide for the Care and Use of Laboratory Animals (National Research Council U.S., 2011).

2.14. Statistical analysis

Statistical Analysis was completed using Prism 7.0d, GraphPad Software (La Jolla, CA). For comparison of virus titers and cytokine concentrations, a two-way analysis of variance (ANOVA) was completed with treatment and day-post-infection as factors. A Dunnett post-test was used to compare guanidine-treated groups to placebo controls. Cytokine differences were evaluated by ANOVA assuming equal variance and normal distribution. For Penh measurements obtained from plethysmography, a two-way ANOVA was completed with treatment and day-post-infection as factors. Both treated and placebo groups were compared to the mock-infected group as a baseline.

3. Results

3.1. Respiratory disease model in four-week-old mice

Guanidine treatment at 200 mg/kg/day significantly reduced lung virus titers in mice infected intranasally with mouse-adapted EV-D68 (Fig. 1A). Significant reductions from placebo-treated mice were observed in mean lung virus titers on day 1 and day 3 post-infection. Guanidine treatment provided a 200-fold reduction (7.3 ± 0.2 vs $5.0 \pm 0.9 \log_{10}$) on day 1 post-infection and a 1600-fold reduction (7.7 ± 0.4 vs $4.5 \pm 1.0 \log_{10}$) on day 3 post-infection compared to placebo-treated mice. Following treatment with 100 mg/kg/day of guanidine, a 20-fold reduction was observed on day 1 (7.3 ± 0.2 vs $6.0 \pm 0.3 \log_{10}$) and day 3 (7.7 ± 0.4 vs $6.4 \pm 2.5 \log_{10}$), however the differences were not statistically significant. The respiratory infection caused by EV-D68 is acute with rapid elevation of virus titers in the lung peaking on day 1–3. Following that peak in virus titer, the virus begins to be cleared from the lung with as much as a two log decrease in titer observed by day 5 post-infection, even in untreated mice. The rapid clearance of virus by day 5 is the reason significant differences between treated and non-treated mice are not observed on that date. Guanidine treatment appears to inhibit virus replication, but does not completely prevent replication. However, prevention of the high virus titers in the lung also prevents virus spread to the blood, limiting or preventing clinical signs of disease.

3.2. Blood virus titers

While virus titers were detected in the blood of placebo-treated mice on days 1 and 3 post-infection, both doses of guanidine decreased blood virus titers significantly (Fig. 1B). This decrease was calculated as a 160-fold reduction (2.9 ± 1.5 vs $< 0.7 \pm 0.0 \log_{10}$) on day 1 and a 2000-fold reduction (4.0 ± 0.0 vs $< 0.7 \pm 0.0 \log_{10}$) on day 3 post-infection.

3.3. Cytokines from lung tissue

Of the 16 cytokines and chemokines evaluated, guanidine treatment significantly reduced concentrations of IL-6 (Fig. 1C) and MCP-1 (Fig. 1D) consistently. Guanidine treatment at both doses significantly reduced concentrations of IL-6 on day 3 post-infection compared to placebo-treated mice. In addition, concentrations of MCP-1 were reduced on day 3 post-infection in both treatment groups and day 5 post-infection in mice treated with 200 mg/kg/day of guanidine. As part of characterizing this model for use in the evaluation of experiment therapeutics, we completed a number of repeat studies to identify variability in our results. A number of other proinflammatory cytokines were elevated in different studies, e.g. RANTES. However, variability observed in other cytokine values prevented us from using them as consistent clinical signs in our disease model. The spikes in IL-6 and MCP-1 were consistently observed in all placebo-treated animals in all studies.

3.4. Histopathology

A moderate interstitial pneumonia characterized by perivascular and alveolar wall infiltration of neutrophils was observed in placebo-treated mice. Three of four placebo-treated mice were observed with mild lesions and the fourth mouse was observed with minimal lung lesions. No lesions were observed in the lungs of mice treated with either 100 or 200 mg/kg/day of guanidine. Treatment with both 100 and 200 mg/kg/day of guanidine reduced inflammation of the lung tissue in EV-D68-infected mice (Fig. 2). Despite modest reductions in lung virus titers, guanidine treatment prevented damage to the lung tissue as quantified by the presence of histological lesions. Since lesions were not observed in the lungs of any guanidine-treated mice, we did not attempted to quantify the lung lesions beyond the scale indicated. However, if partial protection of lungs from histological lesions are observed in future evaluations of experimental drugs, we will develop a lesion scoring system in an attempt to make the lesion scores quantitative.

3.5. Enhanced pause (Penh)

Guanidine treatment reduced the effect of EV-D68 infection on Penh in mice (Fig. 3). Uninfected mice served as a normal baseline for measurements of Penh throughout the study and both guanidine-treated and placebo-treated mice were compared to control mice. A significant increase in Penh (34%), indicative of morbidity, was observed in placebo-treated mice on day 5 post-infection. However, Guanidine-treated mice were not statistically different compared to the normal control mice.

3.6. Neurological disease model in 10-day-old mice

Mice infected intraperitoneally with EV-D68 succumbed to infection based upon the virus dose used for inoculation (Fig. 4A). The mouse-adapted virus caused mortality in 100% of the mice (6/6) using a dose of $1.0 \times 10^{6.7}$ $CCID_{50}$/mouse. A dose of $1.0 \times 10^{6.2}$ EV-D68 $CCID_{50}$/mouse caused mortality in 66% of the mice (4/6) that were infected. Lower doses of $1.0 \times 10^{5.7}$ and $1.0 \times 10^{5.2}$ $CCID_{50}$/mouse of EV-D68 led to mortality in 17% (1/6) of mice for both infectious doses of virus.

Infection with EV-D68 led to observable paralysis in mice that was quantified using an adapted neurological scoring system. The time of onset and severity of paralysis depended upon the infectious dose of virus used for challenge (Fig. 4B). A significant increase in neurological scores was observed on days 3 and 4 post-infection in the group infected with $1.0 \times 10^{6.7}$ $CCID_{50}$/mouse of EV-D68. Paralysis was observed in 100% of mice (6/6) infected with the highest challenge dose. The severity of paralysis increased until the mice succumbed to infection. Paralysis was also observed in 83% of mice (5/6) infected with $1.0 \times 10^{6.2}$ $CCID_{50}$/mouse of EV-D68. While 4 of the 5 mice in which paralysis was observed succumbed to the infection, one mouse recovered from the paralysis and survived the infection. The neurological

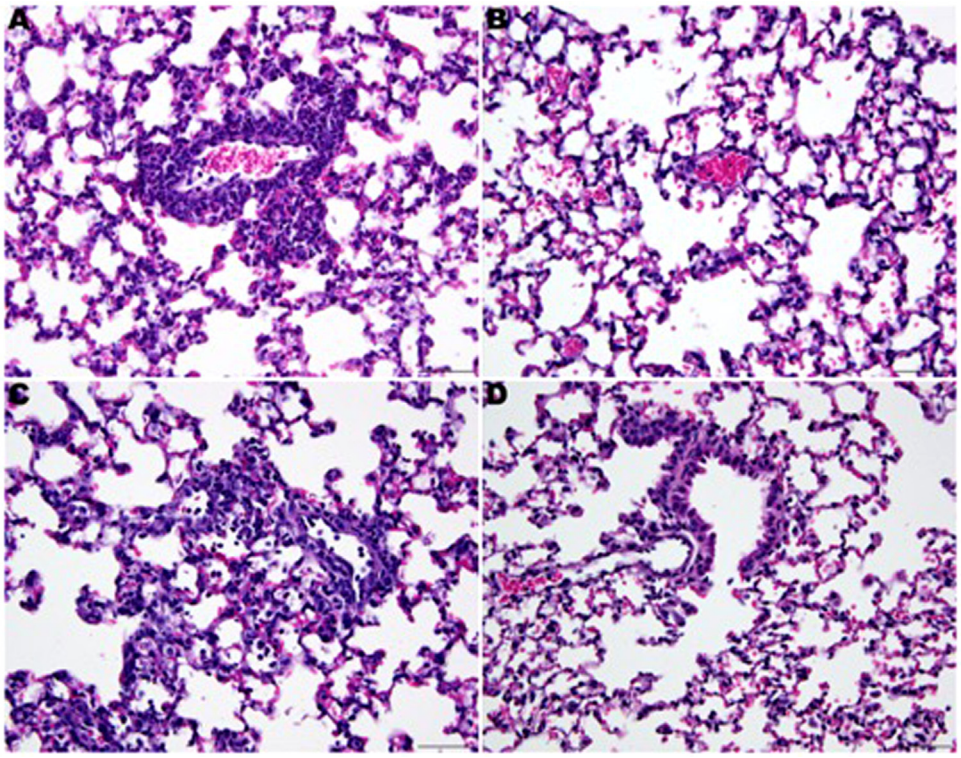

Fig. 2. Histological lesions in lung tissues observed in four-week-old mice infected with EV-D68 and treated with guanidine. Placebo treated mice (A and C). Perivascular infiltration with neutrophils around small and medium sized blood vessels (A) with occasional neutrophils within alveolar spaces (C). Mice treated with guanidine 200 mg/kg/day (B) or 100 mg/kg/day (D). No histologic lesions are present. Hematoxylin-Eosin. 400×.

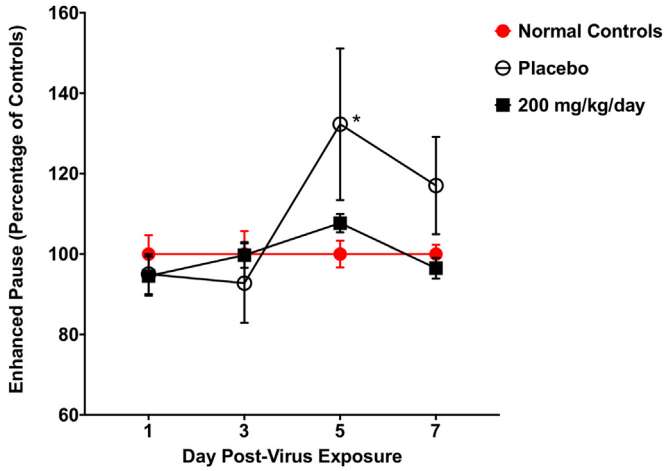

Fig. 3. Enhanced pause (Penh) in four-week-old mice infected intranasally with EV-D68 and treated with guanidine. Mice (n = 8/group) were treated b.i.d. x 5 days beginning 4 h post-infection. Guanidine treatment prevented increases in Penh observed in EV-D68-infected mice. Placebo-treated and guanidine-treated mice were compared to normal controls as a baseline. $^{*}P < 0.05$.

score was significantly higher than control mice on days 4 and 5 post-infection. In addition, paralysis was observed in 50% of mice (3/6) challenged with both of the lower doses of EV-D68. One mouse in each group succumbed to infection but the remaining mice recovered from paralysis and survived to the end of the study.

3.7. In vivo evaluation of guanidine treatment in 10-day-old AG129 mice

Treatment with guanidine protected 10-day-old AG129 mice from mortality (Fig. 5A) and paralysis as indicated by neurological score (Fig. 5B). Guanidine protected 100% of the mice (5/5) from mortality at doses of 50 and 100 mg/kg/day. Doses of either 12.5 or 25 mg/kg/day did not offer protection against mortality. Both higher treatment doses (50 and 100 mg/kg/day) of guanidine protected mice from virus-induced paralysis throughout the study. No paralysis was observed in either treatment group and neurological scores were significantly different from placebo-treated mice on day 3, day 4, and day 5 post-infection. Lower doses of guanidine (12.5 and 25 mg/kg/day) did not provide protection from paralysis and neurological scores were similar to placebo-treated mice.

Guanidine treatment significantly reduced virus titers in every tissue evaluated (Fig. 6). Guanidine treatment significantly reduced virus titers in the lungs (5.2 ± 0.5 vs $2.8 \pm 1.5 \log_{10}$) and virus titers were only detected in 2 of 5 samples from the spinal cord and were not detected in any of the brain tissue samples.

4. Discussion

The outbreak of EV-D68 in 2014 as well as the link to AFM have led to the classification of EV-D68 as a re-emerging disease (Imamura and Oshitani, 2015). Up to this point, clinical intervention has relied mainly on supportive care and relieving patient symptoms. Therapeutic interventions are needed to reduce virus burden and improve disease outcome. A recent publication by Hixon, Clarke and Tyler evaluated the efficacy of human intravenous immunoglobulin (hIVIG), fluoxetine, and dexamethasone in a mouse model of paralytic myelitis (Hixon et al., 2017b). While hIVIG reduced paralysis and spinal cord viral load, fluoxetine had no effect on either parameter and dexamethasone worsened paralysis and viral burden of the spinal cord. While the work of Hixon, Clarke and Tyler is valuable for the data presented on the evaluation of clinically relevant antiviral compounds, they were unable to evaluate the effects of these compounds on respiratory disease (Hixon et al., 2017b). In addition, our model of neurological disease can be evaluated by observation of hind limb paralysis as it develops in the mice after infection. We also observed prevention of that paralysis following antiviral drug treatment. While both two-day-old mice and 10-day-old AG129 mice are immunologically deficient, the increased size of the 10-day-old mice makes administration of antiviral therapies more practical, and these studies in 4-week-old mice represent the first model for the evaluation of antiviral therapies against respiratory

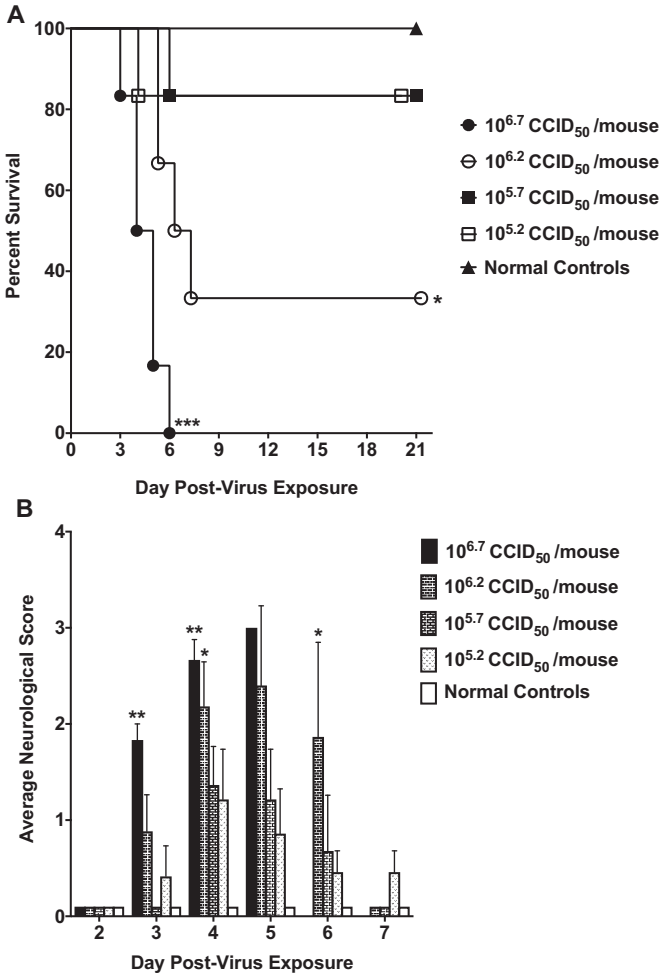

Fig. 4. Survival and average neurological scores for 10-day-old mice infected with EV-D68. Mice (n = 6/group) were infected with half-log dilutions of EV-D68 via the i.p. route. (A) 10-day-old mice were infected with four different doses of EV-D68 via the i.p. route. Survival was dependent on the challenge dose of EV-D68. Significance denotes comparison to normal control mice. (B) Average neurological scores for 10-day-old mice were recorded daily. Paralysis was observed in all infected groups but was more severe in groups challenged with a higher dose of virus. $^{*}P < 0.05$, $^{**}P < 0.01$, $^{***}P < 0.001$.

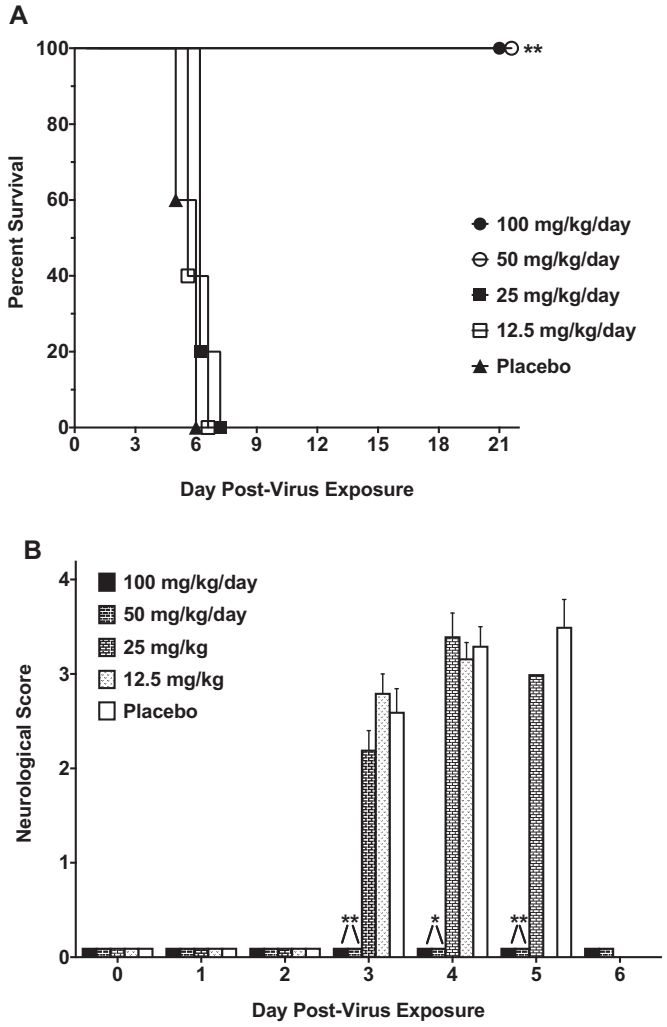

Fig. 5. Survival and mean neurological scores for 10-day-old mice infected with EV-D68 and treated with guanidine. Mice (n = 5/group) were treated b.i.d. × 5 days beginning 4 h post-infection. (A) Guanidine treatment significantly improved survival in 10-day-old mice infected via the i.p route with EV-D68. Lower doses of guanidine did not affect survival or mean day of death. (B) Treatment with guanidine prevented paralysis as measured by decreases in mean neurological scores. $^{*}P < 0.05$, $^{**}P < 0.01$.

disease following EV-D68 infection.

Development of a virus infection model also requires the identification of an antiviral compound that can serve as a positive control. Without the use of a positive control, an experimental drug could fail to protect mice following infection due to over challenge with virus or some other anomaly in the study. However, if the positive control drug performs as expected, it is safer to conclude that the experimental drug did not provide efficacy at the dose and route tested. To identify a positive control for use in our EV-D68 disease models, we evaluated Enviroxime, Pirodivir, Pleconaril, Ribavirin, Rupintravir and guanidine. Each of these compounds showed high antiviral activity in vitro, but only guanidine protected mice from infection in the mouse models. Guanidine decreased lung and blood virus titers in EV-D68-infected mice in the respiratory model. After infection, virus titers peak at approximately 10^8 virus/ml in the lung on day 1–3, then decrease until virus is no longer detectable by day 9. Virus in the blood peaks at approximately 10^6 virus/ml on day 1–3, then decreases by day 5. The virus titer in the lung following guanidine treatment, never increased above 10^6 virus/ml and was not observed in the blood, indicating that guanidine treatment inhibited virus replication. Since guanidine acts on the 2 C protein of EV-D68, it is likely that guanidine prevents replication of EV-D68 (Caliguiri and Tamm, 1968). We hypothesize that the virus initially replicates in the lung and then spreads to blood where the viremia leads to infection of other tissues, including the central nervous system. Guanidine treatment reduced virus replication in the lung, thereby limiting virus spread to the blood. These studies demonstrate that guanidine is an effective positive control drug for use in our EV-D68 infection models in AG129 mice.

Decreased concentrations of IL-6 and MCP-1 in the same lung tissue samples indicated a decrease in tissue inflammation following guanidine treatment. Decreases in IL-6 and MCP-1 and severity of the interstitial pneumonia support the conclusion that inflammation of the lung tissue is lessened by treatment with guanidine.

The CDC summaries report from the EV-D68 outbreaks between 2008 and 2010, and the 2014 U.S. outbreak indicated that EV-D68 may cause severe upper and lower respiratory tract disease (Centers for Disease Control and Prevention CDC, 2011; Midgley et al., 2014). However, the majority of patients had only mild disease with the predominant symptoms of cough and dyspnea (Centers for Disease Control and Prevention CDC, 2011; Midgley et al., 2014). We are not aware of any reports in the literature describing histological lesions following EV-D68 respiratory disease in humans. However, the lesions associated

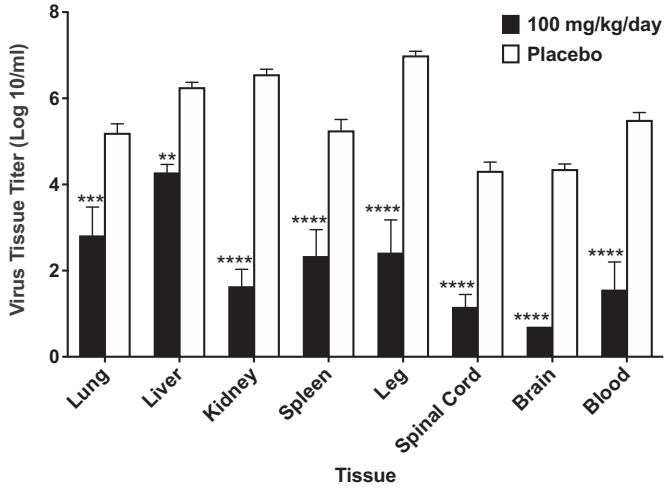

Fig. 6. Virus titers in tissue from 10-day-old mice infected with EV-D68 and treated with guanidine. Mice (n = 5/group) were treated b.i.d. × 5 days beginning 4 h post-infection. Guanidine treatment at 100 mg/kg/day decreased virus tissue titers by at least 2-logs in all tissues that were evaluated. Reductions to virus titers in the spinal cord and brain are likely responsible for increases in survival. $^{**}P < 0.01$, $^{***}P < 0.001$, $^{****}P < 0.0001$.

with interstitial pneumonia caused by EV-D68 in mice are similar to lesions observed in human respiratory infections caused by rhinovirus, respiratory syncytial virus, and rare cases of influenza vaccine-induced lung injury (Jacobs et al., 2013; Imakita et al., 2000; Banna et al., 2004; Hibino and Kondo, 2017).

In this study, guanidine reduced the changes in Penh that were observed in placebo-treated mice. This result agrees with decreases in lung inflammation reflected in the cytokine concentrations and severity of the interstitial pneumonia. However, due to the controversy surrounding Penh, specifically the inappropriate use of Penh as an indicator of airway resistance (Lomask, 2006; Menachery et al., 2015; Lundblad et al., 2007; Bates et al., 2004) we simply consider Penh to be an indicator of morbidity in mice. As Penh was not the primary focus of this paper, we have not attempted to address the controversy surrounding its meaning in animal models. No mortality was observed in the respiratory model following infection, so we were unable to correlate Penh with mortality. However, we suspect that it does identify an effect of virus infection on lung function, although we are unable to make definitive conclusions around the true meaning of Penh. Ongoing studies are attempting to address that meaning in our model of EV-D68 infection.

Guanidine reduced signs of respiratory disease when treatment started 4 hrs post-infection. While it may seem impractical from a clinical standpoint, the +4 h treatment window provides a reasonable expectation of efficacy in an animal model and is stringent enough to eliminate compounds that do not effectively reduce signs of disease after infection. In addition, investigators in the Institute for Antiviral Research at Utah State University have participated in the Collaborative Antiviral Testing Group of the NIH for more than 25 years. During that time, thousands of experimental therapeutics from Sponsors around the world have been evaluated by in vitro testing methods and in animal models. This treatment approach in animal models has been successful in the preclinical development of compounds that were later licensed for clinical use, including ribavirin (Virazole™), stavudine (Zerit™), oseltamivir (Tamiflu™), Peramivir (Rapivab), and T-705 (Favipiravir) (Sidwell et al., 1972, 1992, 1998, 2007; Smee et al., 2001). The data provided in the Supplemental information shows results following evaluation of a number of antiviral compounds that had previously shown promise in vitro against EV-D68, although none of them were effective in our animal model, even when treatment was initiated at +4 h post-infection. Only guanidine was able to significantly reduce signs of disease in the EV-D68 mouse model. Due to its potential toxicity the development of guanidine as a therapeutic was not further evaluated, although it provides a reliable and robust positive control in both respiratory and neurological disease models for EV-D68 infection. Since guanidine is only used as a positive control, we did not evaluate the therapeutic window for guanidine treatment. In addition, we recognize that beginning treatment at 4 h post-infection does not reflect the clinical situation, and thus may provide an over-optimistic estimate of guanidine's antiviral effect in vivo. To determine the therapeutic window in our disease models, we recently completed an evaluation of human intravenous immunoglobulin (IVIg) as treatment for an EV-D68 infection in mice (Peterson et al., 2018). In the respiratory disease model, a single intraperitoneal treatment with IVIg at 24 and 48 h post-infection had little impact on lung virus titers and histopathology in the lungs, but did reduce virus titers in the blood. However, in the neurological disease model, delayed treatment with IVIg until 24 or 48 h p.i. protected 100% and 80% of the mice from mortality, respectively, and prevented paralysis from EV-D68 infection as indicated by decreased neurological scores (Peterson et al., 2018).

Our model of EV-D68 neurological disease in 10-day-old AG129 mice demonstrates a rapid onset of paralysis and mortality following i.p. infection of EV-D68. We previously demonstrated that EV-D68 infection produced an acute flaccid paralysis, including myelitis, myositis, and muscle atrophy at the onset of paralysis in mice. Those data suggest that motor deficits are caused by loss of motor neurons in the spinal cord, but early muscle infection and disease may also contribute to the deficits (Morrey et al., 2018). Guanidine improved survival and decreased paralysis as indicated by neurological scores in treated mice. In addition, treatment with 50 and 100 mg/kg/day of guanidine protected mice from mortality and paralysis. One limitation of our studies is the use of AG129 mice lacking interferon receptors. Since these animals were necessary to observe signs of disease, it is unknown whether compounds identified in our model would be active in mice with an intact interferon response. However, since the antiviral compound does not have the benefit of an interferon response to aid in virus clearance, we believe this creates a stringent model where the antiviral compound must be highly effective in order to limit viral replication and prevent signs of disease.

Guanidine is a well-known compound that has been used for the treatment of Lambert-Eaton myasthenic syndrome, an autoimmune disorder affecting neuromuscular junctions (Lambert, 1966). However, the drug has not been widely used due to toxicity concerns (Lindquist and Stangel, 2011).

Guanidine is an inhibitor of the 2C protein of picornaviruses (Sadeghipour et al., 2012). While the exact function of the 2 C protein is unclear, it is necessary for viral replication and interaction with guanidine inhibits RNA synthesis. Guanidine has previously been used in conjunction with 2-(α-hydroxybenzyl)-benzimidazole to treat paralysis in mice infected with Coxsackievirus A9 (Eggers, 1976). However, these studies represent the first treatment of both respiratory and neurological disease with an antiviral compound in EV-D68-infected mice. While guanidine may treat enterovirus infections in mice, we expect concerns regarding toxicity to prevent clinical applications. Guanidine may serve as a scaffold for the synthesis of future compounds and establishes the 2 C protein as a target for antiviral therapy of EV-D68 infections. In addition, guanidine can be used as the positive control for models of EV-D68 infection.

We developed two models for EV-D68 infection in AG129 mice that respond to treatment with guanidine. For an EV-D68 respiratory infection, four-week-old AG129 mice were infected intranasally with a mouse-adapted strain of EV-D68. Guanidine decreased: lung virus titers, lung cytokine concentrations, and inflammation in the lung. In addition, whole body plethysmography was used to show that guanidine prevented increases in Penh observed in EV-D68-infected mice. This work represents the first respiratory model of EV-D68 infection that responds to antiviral therapy. In the neurological model, guanidine

treatment prevented EV-D68-induced paralysis and mortality establishing guanidine as a functional control for EV-D68 infection in mice. While toxicity may prevent clinical use, guanidine may represent a starting point for drug development. The 2C protein of EV-D68 appears to be a reasonable target for antiviral therapies.

In addition, we evaluated Enviroxime, Pirodivir, Pleconaril, Ribavirin, and Rupintravir in the respiratory and neurological disease models as potential antiviral therapies. However, none of these antiviral compounds showed therapeutic efficacy in our in vivo models (Table S1, Supplementary information). However, we feel that this information is important as many of these compounds have been suggested as potential therapies for EV-D68 infections.

Acknowledgements

This work was done at the Institute for Antiviral Research at Utah State University. Funding was provided by the National Institute of Health contract number HHSN2722010000391, Task Order A79, from the Virology Branch, Division of Microbiology and Infectious Diseases, National Institute of Allergy and Infectious Diseases, National Institutes of Health, USA.

Conflicts of interest

The authors declare no conflict of interest.

Appendix A. Supporting information

Supplementary data associated with this article can be found in the online version at doi:10.1016/j.virol.2018.10.014.

References

Aliabadi, N., Messacar, K., Pastula, D.M., Robinson, C.C., Leshem, E., Sejvar, J.J., Nix, W.A., Oberste, M.S., Feikin, D.R., Dominguez, S.R., 2016. Enterovirus D68 infection in children with acute flaccid myelitis, Colorado, USA, 2014. Emerg. Infect. Dis. 22, 1387–1394.

Banna, G.L., Aversa, S.M., Cattelan, A.M., Crivellari, G., Monfardini, S., 2004. Respiratory syncytial virus-related pneumonia after stem cell transplantation successfully treated with palivizumab and steroid therapy. Scand. J. Infect. Dis. 36, 155–157.

Bates, J., Irvin, C., Brusasco, V., Drazen, J., Fredberg, J., Loring, S., Eidelman, D., Ludwig, M., Macklem, P., Martin, J., Milic-Emili, J., Hantos, Z., Hyatt, R., Lai-Fook, S., Leff, A., Solway, J., Lutchen, K., Suki, B., Mitzner, W., Pare, P., Pride, N., Sly, P., 2004. The use and misuse of Penh in animal models of lung disease. Am. J. Respir. Cell Mol. Biol. 31, 373–374.

van den Broek, M.F., Muller, U., Huang, S., Aguet, M., Zinkernagel, R.M., 1995. Antiviral defense in mice lacking both alpha/beta and gamma interferon receptors. J. Virol. 69, 4792–4796.

Caliguiri, L.A., Tamm, I., 1968. Action of guanidine on the replication of poliovirus RNA. Virology 35, 408–417.

Centers for Disease Control and Prevention (CDC), 2011. Clusters of acute respiratory illness associated with human enterovirus 68—Asia, Europe, and United States, 2008–2010. MMWR Morb. Mortal. Wkly. Rep. 60, 1301–1304.

Control CfD, July 19, 2016 2017. Enterovirus D68. ⟨https://www.cdc.gov/non-polio-enterovirus/about/ev-d68.html⟩. (Accessed 22 May 2017).

Crone, M., Tellier, R., Wei, X.C., Kuhn, S., Vanderkooi, O.G., Kim, J., Mah, J.K., Mineyko, A., 2016. Polio-like illness associated with outbreak of upper respiratory tract infection in children. J. Child Neurol. 31, 409–414.

Eggers, H.J., 1976. Successful treatment of enterovirus-infected mice by 2-(alpha-hydroxybenzyl)-benzimidazole and guanidine. J. Exp. Med. 143, 1367–1381.

Esposito, S., Bosis, S., Niesters, H., Principi, N., 2015. Enterovirus D68 infection. Viruses 7, 6043–6050.

Esposito, S., Chidini, G., Cinnante, C., Napolitano, L., Giannini, A., Terranova, L., Niesters, H., Principi, N., Calderini, E., 2017. Acute flaccid myelitis associated with enterovirus-D68 infection in an otherwise healthy child. Virol. J. 14, 4.

Evans W.J., Hurst, B.L., Peterson, C.J., Van Wettere, A., Day, C.W., Smee, D.F., Tarbet, E. B. Development of a Respiratory Disease Model for Enterovirus D68 in 4-Week-Old Mice for Evaluation of Antiviral Therapies (manuscript submitted for publication).

Gowen, B.B., Wong, M.H., Larson, D., Ye, W., Jung, K.H., Sefing, E.J., Skirpstunas, R., Smee, D.F., Morrey, J.D., Schneller, S.W., 2010. Development of a new tacaribe arenavirus infection model and its use to explore antiviral activity of a novel aristeromycin analog. PLoS One 5 (9), e12760.

Greninger, A.L., Naccache, S.N., Messacar, K., Clayton, A., Yu, G., Somasekar, S., Federman, S., Stryke, D., Anderson, C., Yagi, S., Messenger, S., Wadford, D., Xia, D., Watt, J.P., Van Haren, K., Dominguez, S.R., Glaser, C., Aldrovandi, G., Chiu, C.Y., 2015. A novel outbreak enterovirus D68 strain associated with acute flaccid myelitis cases in the USA (2012-14): a retrospective cohort study. Lancet Infect. Dis. 15, 671–682.

Hatzipetros, T., Kidd, J.D., Moreno, A.J., Thompson, K., Gill, A., Vieira, F.G., 2015. A quick phenotypic neurological scoring system for evaluating disease progression in the SOD1-G93A mouse model of ALS. J. Vis. Exp. https://doi.org/10.3791/53257.

Hibino, M., Kondo, T., 2017. Interstitial pneumonia associated with the influenza vaccine: a report of two cases. Intern. Med. 56, 197–201.

Hixon, A.M., Yu, G., Leser, J.S., Yagi, S., Clarke, P., Chiu, C.Y., Tyler, K.L., 2017a. A mouse model of paralytic myelitis caused by enterovirus D68. PLoS Pathog. 13, e1006199.

Hixon, A.M., Clarke, P., Tyler, K.L., 2017b. Evaluating treatment efficacy in a mouse model of enterovirus D68-associated paralytic myelitis. J. Infect. Dis. 216, 1245–1253.

Hovden, I.A., Pfeiffer, H.C., 2015. Electrodiagnostic findings in acute flaccid myelitis related to enterovirus D68. Muscle Nerve 52, 909–910.

Imakita, M., Shiraki, K., Yutani, C., Ishibashi-Ueda, H., 2000. Pneumonia caused by rhinovirus. Clin. Infect. Dis. 30, 611–612.

Imamura, T., Oshitani, H., 2015. Global reemergence of enterovirus D68 as an important pathogen for acute respiratory infections. Rev. Med. Virol. 25, 102–114.

Jacobs, S.E., Soave, R., Shore, T.B., Satlin, M.J., Schuetz, A.N., Magro, C., Jenkins, S.G., Walsh, T.J., 2013. Human rhinovirus infections of the lower respiratory tract in hematopoietic stem cell transplant recipients. Transpl. Infect. Dis. 15, 474–486.

Julander, J.G., Siddharthan, V.J., 2017. Small-animal models of Zika Virus. Infect. Dis. 216 (Suppl 10), S919–S927.

Julander, J.G., Perry, S.T., Shresta, S., 2011. Important advances in the field of anti-dengue virus research. Antivir. Chem. Chemother. 21 (3), 105–116.

Lambert, E.H., 1966. Defects of neuromuscular transmission in syndromes other than myasthenia gravis. Ann. N.Y. Acad. Sci. 135, 367–384.

Lang, M., Mirand, A., Savy, N., Henquell, C., Maridet, S., Perignon, R., Labbe, A., Peigue-Lafeuille, H., 2014. Acute flaccid paralysis following enterovirus D68 associated pneumonia, France, 2014. Eur. Surveill. 19.

Lindquist, S., Stangel, M., 2011. Update on treatment options for Lambert-Eaton myasthenic syndrome: focus on use of amifampridine. Neuropsychiatr. Dis. Treat. 7, 341–349.

Lomask, M., 2006. Further exploration of the Penh parameter. Exp. Toxicol. Pathol. 57 (Suppl 2), 13–20.

Lundblad, L.K., Irvin, C.G., Hantos, Z., Sly, P., Mitzner, W., Bates, J.H., 2007. Penh is not a measure of airway resistance!. Eur. Respir. J. 30, 805.

Maloney, J.A., Mirsky, D.M., Messacar, K., Dominguez, S.R., Schreiner, T., Stence, N.V., 2015. MRI findings in children with acute flaccid paralysis and cranial nerve dysfunction occurring during the 2014 enterovirus D68 outbreak. AJNR Am. J. Neuroradiol. 36, 245–250.

Menachery, V.D., Gralinski, L.E., Baric, R.S., Ferris, M.T., 2015. New metrics for evaluating viral respiratory pathogenesis. PLoS One 10, e0131451.

Messacar, K., Schreiner, T.L., Maloney, J.A., Wallace, A., Ludke, J., Oberste, M.S., Nix, W.A., Robinson, C.C., Glode, M.P., Abzug, M.J., Dominguez, S.R., 2015. A cluster of acute flaccid paralysis and cranial nerve dysfunction temporally associated with an outbreak of enterovirus D68 in children in Colorado, USA. Lancet 385, 1662–1671.

Messacar, K., Abzug, M.J., Dominguez, S.R., 2016a. 2014 outbreak of enterovirus D68 in North America. J. Med. Virol. 88, 739–745.

Messacar, K., Hawkins, S.M., Baker, J., Pearce, K., Tong, S., Dominguez, S.R., Parker, S., 2016b. Resource burden during the 2014 Enterovirus D68 respiratory disease outbreak at Children's Hospital Colorado: an unexpected strain. JAMA Pediatr. 170, 294–297.

Midgley, C.M., Jackson, M.A., Selvarangan, R., Turabelidze, G., Obringer, E., Johnson, D., Giles, B.L., Patel, A., Echols, F., Oberste, M.S., Nix, W.A., Watson, J.T., Gerber, S.I., 2014. Severe respiratory illness associated with enterovirus D68— Missouri and Illinois, 2014. MMWR Morb. Mortal. Wkly. Rep. 63, 798–799.

Mirand, A., Peigue-Lafeuille, H., 2015. Acute flaccid myelitis and enteroviruses: an ongoing story. Lancet 385, 1601–1602.

Morrey, J.D., Wang, H., Hurst, B.L., Zukor, K., Siddharthan, V., Van Wettere, A.J., Sinex, D.G., Tarbet, E.B., 2018. Causation of acute flaccid paralysis by myelitis and myositis in enterovirus-D68 infected mice deficient in interferon alphabeta/gamma receptors. Viruses 10 (1) (pii: E33).

Muller, U., Steinhoff, U., Reis, L.F., Hemmi, S., Pavlovic, J., Zinkernagel, R.M., Aguet, M., 1994. Functional role of type I and type II interferons in antiviral defense. Science 264, 1918–1921.

National Research Council (U.S.), 2011. Committe for the Update of the Guide for the Care and Use of Laboratory Animals IfLARUS, National Academies Press (U.S.). Guide for the care and use of Laboratory Animals National Academies Press.

Nelson, G.R., Bonkowsky, J.L., Doll, E., Green, M., Hedlund, G.L., Moore, K.R., Bale Jr., J.F., 2016. Recognition and management of acute flaccid myelitis in children. Pediatr. Neurol. 55, 17–21.

Peterson C.J., Hurst, B.L., Evans, W.J., Smee, D.F., Tarbet E.B., 2018. Evaluation of human intravenous immunoglobulin in disease models of EV-D68 and EV-71 infections in mice (manuscript submitted for publication).

Pfeiffer, H.C., Bragstad, K., Skram, M.K., Dahl, H., Knudsen, P.K., Chawla, M.S., Holberg-Petersen, M., Vainio, K., Dudman, S.G., Kran, A.M., Rojahn, A.E., 2015. Two cases of acute severe flaccid myelitis associated with enterovirus D68 infection in children, Norway, autumn 2014. Eur. Surveill. 20, 21062.

Reed, L.M., H., 1938. A simple method of estimating fifty percent endpoints. Am. J. Hyg. 27, 493–497.

Rui, Y., Su, J., Wang, H., Chang, J., Wang, S., Zheng, W., Cai, Y., Wei, W., Gordy, J.T., Markham, R., Kong, W., Zhang, W., Yu, X.F., 2017. Disruption of MDA5-mediated innate immune responses by the 3C proteins of Coxsackievirus A16, Coxsackievirus

A6, and Enterovirus D68. J. Virol. 91.
Sadeghipour, S., Bek, E.J., McMinn, P.C., 2012. Selection and characterisation of guanidine-resistant mutants of human enterovirus 71. Virus Res. 169, 72–79.
Sarathy, V.V., Milligan, G.N., Bourne, N., Barrett, A.D., 2015. Mouse models of dengue virus infection for vaccine testing. Vaccine 33 (50), 7051–7060.
Sidwell, R.W., Huffman, J.H., Khare, G.P., Allen, L.B., Witkowski, J.T., Robins, R.K., 1972. Broad-spectrum antiviral activity of Virazole: 1-beta-d-ribofuranosyl-1,2,4-triazole-3-carboxamide. Science 177, 705–706.
Sidwell, R.W., Hitchcock, M., Okleberry, K.M., Burger, R.A., Warren, R.P., Morrey, J.D., 1992. Suppression of murine retroviral disease by 2′,3′-didehydro-2′,3′-dideoxythymidine (D4T). Antivir. Res. 19, 313–324.
Sidwell, R.W., Huffman, J.H., Barnard, D.L., Bailey, K.W., Wong, M.H., Morrison, A., Syndergaard, T., Kim, C.U., 1998. Inhibition of influenza virus infections in mice by GS4104, an orally effective influenza virus neuraminidase inhibitor. Antivir. Res. 37, 107–120.
Sidwell, R.W., Barnard, D.L., Day, C.W., Smee, D.F., Bailey, K.W., Wong, M.H., Morrey, J.D., Furuta, Y., 2007. Efficacy of orally administered T-705 on lethal avian influenza A (H5N1) virus infections in mice. Antimicrob. Agents Chemother. 51, 845–851.
Smee, D.F., Huffman, J.H., Morrison, A.C., Barnard, D.L., Sidwell, R.W., 2001. Cyclopentane neuraminidase inhibitors with potent in vitro anti-influenza virus activities. Antimicrob. Agents Chemother. 45, 743–748.
Smee, D.F., Evans, W.J., Nicolaou, K.C., Tarbet, E.B., Day, C.W., 2016. Susceptibilities of enterovirus D68, enterovirus 71, and rhinovirus 87 strains to various antiviral compounds. Antivir. Res. 131, 61–65.
Tangermann, R.H., Lamoureux, C., Tallis, G., Goel, A., 2017. The critical role of acute flaccid paralysis surveillance in the Global Polio Eradication Initiative. Int. Health 9, 156–163.
Varghese, R., Iyer, A., Hunter, K., Cargill, J.S., Cooke, R.P., 2015. Sampling the upper respiratory tract for enteroviral infection is important in the investigation of an acute neurological illness in children. Eur. J. Paediatr. Neurol. 19, 494–495.
Williams, C.J., Thomas, R.H., Pickersgill, T.P., Lyons, M., Lowe, G., Stiff, R.E., Moore, C., Jones, R., Howe, R., Brunt, H., Ashman, A., Mason, B.W., 2016. Cluster of atypical adult Guillain-Barre syndrome temporally associated with neurological illness due to EV-D68 in children, South Wales, United Kingdom, October 2015 to January 2016. Eur. Surveill. 21.
World Health Organization, Department of Vaccines and Other Biologicals, 2003. WHO-Recommended Standards for Surveillance of Selected Vaccine-preventable Diseases. Dept. of Vaccines and Biologicals, Health Technology and Pharmaceuticals, World Health Organization, Geneva.
Xiang, Z., Li, L., Lei, X., Zhou, H., Zhou, Z., He, B., Wang, J., 2014. Enterovirus 68 3C protease cleaves TRIF to attenuate antiviral responses mediated by Toll-like receptor 3. J. Virol. 88, 6650–6659.
Xiang, Z., Liu, L., Lei, X., Zhou, Z., He, B., Wang, J., 2015. 3C Protease of Enterovirus D68 inhibits cellular defense mediated by interferon regulatory factor 7. J. Virol. 90, 1613–1621.
Yea, C., Bitnun, A., Robinson, J., Mineyko, A., Barton, M., Mah, J.K., Vajsar, J., Richardson, S., Licht, C., Brophy, J., Crone, M., Desai, S., Hukin, J., Jones, K., Muir, K., Pernica, J.M., Pless, R., Pohl, D., Rafay, M.F., Selby, K., Venkateswaran, S., Bernard, G., Yeh, E.A., 2017. Longitudinal outcomes in the 2014 acute flaccid paralysis cluster in Canada. J. Child Neurol. 32, 301–307.